

# Lowered Nonextensive Stellar Distribution

J. M. Silva<sup>1</sup>, R. E. de Souza<sup>2</sup> and J. A. S. Lima<sup>3</sup>

*Departamento de Astronomia, Universidade de São Paulo, USP, 05508-900 São Paulo, SP, Brazil*

---

## Abstract

The structure of globular clusters and elliptical galaxies are described in an unified way through a new class of lowered models inspired on the nonextensive kinetic theory. These power law models are specified by a single parameter  $q$  which quantifies to what extent they depart from the class of lowered stellar distributions discussed by Michie and King. For  $q = 1$  the Michie-King profiles are recovered. However, for  $q < 1$  there is a gradual modification in the shape of the density profiles which depends on the degree of tidal damage imposed on the model, thereby also providing a good fit for globular clusters. It is also shown that a subclass of these models, those with a deeper potential and  $q$  slightly less than 1, present a distribution resembling the de Vaucoulers  $r^{1/4}$  profile which yields a good description of the structure of elliptical galaxies. This subset of models follows this trend, with a slight departure over nearly 10 orders of magnitudes.

*Key words:* Stellar Dynamics, Nonextensivity, Distribution Function

---

## 1 Introduction

It is widely known that the Maxwell-Boltzmann isothermal distribution is somewhat truncated by the galactic tidal field responsible for the capture of stars that become loosely bound to the main structure. This means that the ideal distribution function (DF) is depopulated due to the stars escaping from the system. As shown by Michie (Michie 1961; Michie 1963a; Michie 1963b; Michie 1963c; Michie 1963d) to the case of non-rotating, spherically symmetric systems, the resulting distribution may be obtained by solving the Fokker-Planck equation. This class of distributions were rediscussed by King (King 1966; King 1965; King 1978; King 1981; King 1962) who showed that

---

<sup>1</sup> jmsilva@astro.iag.usp.br

<sup>2</sup> ronaldo@astro.iag.usp.br

<sup>3</sup> limajas@astro.iag.usp.br

they give a good representation for the observed density profiles of globular clusters (GC). The phase space density for such models may be expressed as (Michie 1963a; Michie 1963b; Michie 1963c; Michie 1963d; Spitzer 1987; Binney & Tremaine 1994)

$$\begin{aligned} f(\varepsilon) &= \rho_o(2\pi\sigma^2)^{-3/2} [e^{-\varepsilon} - 1] & \varepsilon < 0 \\ f(\varepsilon) &= 0 & \varepsilon \geq 0 \end{aligned} \quad (1)$$

where the dimensionless quantity  $\varepsilon = (\frac{1}{2}v^2 + \Phi(\mathbf{r}))/\sigma^2$  is the energy of any given star in units of the average thermal energy ( $\Phi$  is the gravitational potential and  $\sigma$  is the velocity dispersion). Actually, in the case of GC, some independent numerical analysis (Hodge & Michie 1969; Peterson & King 1975; Peterson 1976) have confirmed the quantitative support provided by such distributions usually called lowered models in the literature.

Unfortunately, these Michie-King models do not describe many elliptical galaxies whose smoothness and symmetry are even more striking than those presented by GC. Actually, instead of a specific lowered distribution, the profiles of some giant elliptical galaxies are very well described by the de Vaucouleurs  $r^{1/4}$  law which provides sometimes a remarkable fit over 10 orders of magnitudes of surface brightness, see for instance, (de Vaucouleurs & Capaccioli 1979). Conversely, there are also some elliptical galaxies (like NGC 4472) that are not fitted by the de Vaucouleurs law as they are by the lowered Michie-King models. Such a state of affairs is quite uncomfortable both from a methodological and a physical viewpoint. In particular, it opens a large window for adjusting mechanisms whose primary objective is somewhat explain the existence of individual profiles even for the spherically symmetrical case.

On the other hand, an increasing attention has been paid to possible nonextensive effects in the fields of kinetic theory and statistical mechanics (see <http://tsallis.cat.cbpf.br/biblio.htm> for a regularly updated bibliography on this subject). The main motivation is the lack of a comprehensive treatment including gravitational and Coulombian fields, or more generally, any long range interaction for which the assumed additivity of the entropy present in the standard approach is not valid. Inspired on such problems, Tsallis proposed the following  $q$ -parameterized nonextensive entropic expression (Tsallis 1988)

$$S_q = k_B \frac{[1 - \sum_i p_i^q]}{(q - 1)} \quad , \quad (2)$$

where  $k_B$  is the standard Boltzmann constant,  $p_i$  is the probability of the  $i$ -th microstate, and  $q$  is a parameter quantifying the degree of nonextensivity. In

the limit  $q = 1$  the standard extensive formula, namely

$$S = -k_B \sum_i p_i \ln p_i \quad , \quad (3)$$

is recovered. One the most relevant properties of Tsallis' nonextensive entropy is its pseudoadditivity. Given a composite system  $A + B$ , constituted by two subsystems  $A$  and  $B$ , which are independent in the sense of factorizability of the microstate probabilities, the Tsallis measure verifies  $S_q(A + B) = S_q(A) + S_q(B) + (1 - q)k_B^{-1}S_q(A)S_q(B)$ , which in the limit  $q \rightarrow 1$ ,  $S_q$  reduces to the standard logarithmic measure, and the usual additivity of the extensive statistical mechanics is recovered. In other words,  $|q - 1|$  is a measure of the lack of extensivity of the system.

Later on, the first attempts for exploring the kinetic route associated to Tsallis entropy approach appeared in the literature. The original kinetic derivation advanced by Maxwell (Maxwell 1860) was generalized to include power law distributions as required by this enlarged framework (Sau *et al.* 2001; Scarfone *et al.* 2008; Jiulin 2007; Silva *et al.* 1998). In particular, it was shown that the equilibrium velocity  $q$ -distribution is given by

$$f(v) = B_q \left[ 1 - (1 - q) \frac{mv^2}{2k_B T} \right]^{1/(1-q)} \quad , \quad (4)$$

where the  $B_q$  is a  $q$ -dependent normalization constant which reduces to the Maxwellian value for  $q = 1$ . As shown in (Silva *et al.* 1998), the above distribution is uniquely determined from two simple requirements: (i) isotropy of the velocity space, and (ii) a suitable nonextensive generalization of the Maxwell factorizability condition, or equivalently, the assumption that  $F(v) \neq f(v_x)f(v_y)f(v_z)$ . More recently, the kinetic foundations of the above distribution were investigated in a deeper level through the generalized Boltzmann's transport equation (Lima *et al.* 2001) which incorporated the nonextensive effects using two different ingredients. First, a new functional form to the kinetic local gas entropy, and, second, a nonfactorizable distribution function for the colliding pairs of particles whose physical meaning is quite clear: the Boltzmann chaos molecular hypothesis is not valid in this extended framework. It was also shown that the kinetic version of the Tsallis entropy satisfies an  $H_q$ -theorem, and more important still, the  $q$ -parameterized class of power law velocity distributions emerged as the unique nonextensive solution describing the equilibrium states.

In the astrophysical context, the nonextensive equilibrium velocity distribution related to Tsallis' statistics has been applied to stellar collisionless systems (Plastino & Plastino 1993) to the peculiar velocity function of galaxies clusters (Lavagno *et al.* 1998), as well in studies of gravothermal instability

(Taruya & Sakagami 2002). More recently, we have determined the radial and projected density profiles for two large classes of isothermal stellar systems with basis on the equilibrium power law  $q$ -distributions (Lima & de Souza 2005). Such models are based in the following phase space density

$$f(\epsilon) = \frac{\rho_o C_q}{(2\pi\sigma^2)^{3/2}} [1 - (1 - q)\epsilon]^{1/(1-q)} \quad (5)$$

where the  $q$ -parameter quantifies the nonadditivity property of the gas entropy. For generic values of  $q \neq 1$ , this DF is a power law, whereas for  $q = 1$  it reduces to the standard Maxwell-Boltzmann distribution function. Formally, this result follows directly from the known identity  $\lim_{d \rightarrow 0} (1 + dy)^{\frac{1}{d}} = \exp(y)$  as can be seen in (Abramowitz & Stegun 1972). The quantity  $C_q$  is a  $q$ -dependent normalization constant given by (Lima *et al.* 2002)

$$C_q = (1 - q)^{1/2} \left( \frac{5 - 3q}{2} \right) \left( \frac{3 - q}{2} \right) \frac{\Gamma(\frac{1}{2} + \frac{1}{1-q})}{\Gamma(\frac{1}{1-q})} \quad q \leq 1 \quad (6)$$

and

$$C_q = (q - 1)^{3/2} \left( \frac{3q - 1}{2} \right) \frac{\Gamma(\frac{1}{1-q})}{\Gamma(\frac{1}{1-q} - \frac{3}{2})} \quad q \geq 1, \quad (7)$$

which reduce to the expected result in the limit  $q = 1$ .

With basis on the ideas of Michie (Michie 1961; Michie 1963a; Michie 1963b; Michie 1963c; Michie 1963d) and King (King 1966; King 1965; King 1978; King 1981; King 1962), in this work we propose a new class of lowered nonextensive models which are naturally associated with the above equilibrium distribution. It will be explicitly assumed that the nonextensive isothermal  $q$ -distribution discussed by (Lima *et al.* 2002) cannot strictly be attained for a real stellar system due to the presence of tidal effects with the mean local gravitational field, stellar encounters or any other relaxation mechanism. This means that such mechanisms must gradually modify the ideal velocity distribution in such a way that the final distribution drop to zero at a finite velocity. Hence, one may suppose that the stellar system approaches as far as it can to a quasi power law final state which collectively can be termed nonextensive lowered spheres. As we shall see, this new class of models may potentially describe both classes of spherically symmetric systems, namely globular clusters and elliptical galaxies, thereby reinforcing the possibility that nonextensive effects may have a considerable importance in the astrophysical domain.

The paper is organized as follows. Next section we set up the basic equations defining the lowered nonextensive models. In section III we discuss a large

class of density profiles obtained through a numerical solution of the Poisson equation. Although reproducing the Michie-King models exactly for  $q \rightarrow 1$ , we show that for  $q$  smaller than unity the standard profiles are moderately modified, and therefore, they also provide a good representation for the structure of GC. In section IV we discuss a specific  $q$ -lowered model characterized by a relatively deep central potential. It resembles the de Vaucouleurs law being therefore potentially useful to describe the structure of elliptical galaxies. This model has an extra bonus: it predicts the existence of small fluctuations similar to those appearing in the profiles of early type galaxies, as recently discussed by Caon (Caon *et al.* 1997) based on the Sérsic  $r^{1/n}$  law. Finally, a summary and the main conclusions are presented in section V.

## 2 Lowered Nonextensive Stellar Distribution

Let us now consider a class of lowered nonextensive  $q$ -distribution defined by

$$\begin{aligned} f(\varepsilon) &= \frac{\rho_o C_q}{(2\pi\sigma^2)^{3/2}} \left[ (1 - (1 - q)\varepsilon)^{1/(1-q)} - 1 \right] & \varepsilon < 0 \\ f(\varepsilon) &= 0 & \varepsilon \geq 0 \end{aligned} \quad (8)$$

which arises naturally from our earlier adoption of the isothermal power law distribution to the unperturbed collisionless system (cf. equations (1) and (2)). This means that to the accuracy of the Michie-King approximation, the above distribution is the simplest nonextensive extension representing the steady state solution of the Fokker-Planck equation. The corresponding mass density profile can be obtained by integrating this distribution over the whole possible energy interval. It thus follows that the density profile is given by the expression

$$\rho = \frac{2\rho_o C_q}{\sqrt{\pi}} \int_{\phi}^0 \left[ (1 - (1 - q)\varepsilon)^{\frac{1}{1-q}} - 1 \right] (\varepsilon - \phi)^{1/2} d\varepsilon \quad (9)$$

where  $\phi = \Phi/\sigma^2$  is the dimensionless potential, and the integration limits have been defined by keeping in mind that only bounded objects are present in the stellar distribution. Once again, this expression asymptotically approaches the lowered Michie-King models when  $q \rightarrow 1$ . This expression linking the mass density to the gravitational potential does not have a closed analytical form and therefore must be numerically integrated. Now, in order to simplify the numerical algorithm, it proves convenient to introduce the variable,  $\varepsilon = \chi\phi$ , with (6) assuming the form

$$\rho = \frac{2\rho_o C_q}{\sqrt{\pi}} (-\phi)^{3/2} \int_0^1 \left[ (1 - (1 - q)\phi\chi)^{\frac{1}{1-q}} - 1 \right] (1 - \chi)^{\frac{1}{2}} d\chi \quad (10)$$

which is more amenable to be solved by numerical discretization. Another benefit from this expression is that we can easily verify that the relation between the mass density and the gravitational potential has two asymptotic regimes. In the first limit, when  $\phi \simeq 0$ , we are close to the external surface and we can expand the power expression appearing inside the brackets using the binomial expansion to obtain

$$\rho \simeq \frac{8\rho_o C_q}{15\sqrt{\pi}} (-\phi)^{5/2} \quad \phi \simeq 0 \quad (11)$$

showing that the external structure of these models correspond to a polytropic sphere with Lane-Emden index  $n = 5/2$ . In fact for  $-\phi \geq 1$  this expression gives a good representation of the model as we can verify from Figure 1. In the internal structure we can find another regime in those regions where the gravitational potential is sufficiently large so that  $(1 - q)\phi\chi \gg 1$  in which case,

$$\rho \propto (-\phi)^{\frac{5-3q}{2(1-q)}} \quad (12)$$

showing that in this limit the internal structure is also described by a polytropic sphere whose Lane-Emden index,  $n = (5 - 3q)/2(1 - q)$ , depends on the nonextensive parameter. In fact as showed by Lima *et al.* (Lima *et al.* 2002), the nonextensive isothermal distributions have a profile density corresponding exactly to this polytropic structure. Therefore, in those models where the central potential is sufficiently deep, the internal structure is closely described by this approximation. In particular, we can verify that the model  $q = 5/7$  corresponds to a polytropic sphere with  $n = 5$  which is the limiting case dividing the Lane-Emden family in a branch having finite mass and radius from those having infinite radius and mass. Therefore, in the absence of tidal truncation, models satisfying the restriction  $5/7 < q \leq 1$  have infinite mass and infinite radius and are the ones that we will give more attention below. We can also see that when  $q = 0$  the whole structure is exactly represented by a  $n = 5/2$  polytropic sphere. In figure 1 we show dependence of the mass density as a function of the gravitational potential for a set of representative values of the  $q$  index. We can see from this plot that in the general case the whole structure can be described as the result of a smooth transition between  $n = 5/2$  at the external region to an internal region having  $n = (5 - 3q)/2(1 - q)$ . As happens in the Michie-King models, the value of the central potential is also arbitrarily set to define implicitly the total mass and the external radius. Therefore, only objects with a sufficiently deep gravitational potential have the ability to show the very internal limiting polytropic structure. In all the other cases the

internal region falls in the transition regime where the external polytropic is gently changing towards the asymptotic internal limit. In certain sense, this characteristic is responsible by the variety of density profiles found in these models.

### 3 The Integrated Density Profiles

Having obtained the density as a function of the gravitational potential we can proceed by solving the Poisson equation which provides our dynamical link to obtain the density profile. Following King (King 1966; King 1965; King 1978; King 1981; King 1962) we normalize the density to its central value  $\rho_0$  and introduce a core radius defined as

$$r_c = \frac{9\sigma^2}{4\pi G\rho_0}, \quad (13)$$

that will be used as a unit to measure the radial distance. In the normalized radial coordinate, the Poisson equation becomes

$$\frac{1}{r^2} \frac{d}{dr} r^2 \frac{d\phi}{dr} = 9\varrho \quad (14)$$

where the dimensionless density  $\varrho = \rho(\phi)/\rho(\phi_0)$  can directly be obtained from the solution of Equation (10) for each choice of the parameter  $\phi_0$ , whose value will fix the whole structure of each model.

The Poisson equation can numerically be solved by imposing the boundary conditions  $\phi = \phi_0$  and  $d\phi/dr = 0$  at the origin  $r = 0$ . The solution proceed from the center and stop at the external surface where  $r = r_t$  and  $\phi = \varrho = 0$ . The external and the core radii define naturally a concentration index  $C = r_t/r_c$  indicating how important is the truncation effect due to tidal field. Models with low values of  $C$  correspond to structures where the tidal field had imposed a severe damage to the unperturbed structure. In figure 2 we present a set of solutions for three values of  $q$ . In the upper panel we show the  $q = 1$  model, corresponding to the usual class of lowered Michie-King models. In the other two panels we present the profiles for  $q = 0.9$  and  $q = 0.8$ , showing that models with the same extent of the standard lowered models have different density profiles. Note that all curves have zero gradient for sufficiently small values of  $r$  regardless of the value of  $q$ . Indeed, such a behavior is more noticeable for smaller values of  $q$ . In figure 3 we present the projected density profile for each model presented in figure 2. Assuming that light traces mass these profiles should directly be compared with the surface brightness profiles.

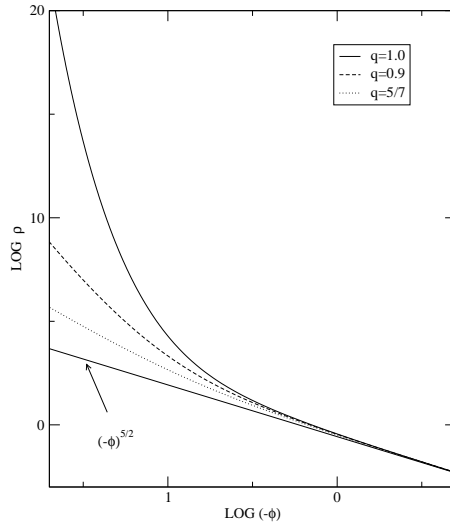


Fig. 1. The density profiles as a function of the gravitational potential has two regimes. In the external region the structure is approximately described by a  $n = 5/2$  polytropic index for all models. In the central region of those objects having a deep potential, the limiting structure depends explicitly on the nonextensive parameter, and resembles a polytropic with  $n = (5 - 3q)/2(1 - q)$ .

The total mass of the  $q$ -lowered models can be evaluated by integrating the density profile as

$$M = 4\pi r_c^3 \rho_o \int_0^C \varrho r^2 dr = 4\pi r_c^3 \rho_o \mu, \quad (15)$$

where  $\mu$  is a dimensionless mass indicator which can be obtained through numerical integration. From Tables 1 and 2 we can see that models with lower concentration  $C$  representing severely damaged structures tend to show a mass distribution close to an uniform spheres with  $\mu = 1/3$ . On the contrary, in objects with higher concentration index the mass is heavily dependent on the central core distribution. In the course of the numerical solution the integration begins by defining an arbitrary value for the central potential  $\phi_0$  and carrying out the integration to a null value at the external surface. However, since we have estimated the total mass we may use its value for determining the gravitational potential at the external surface  $-GM/r_t$  which can be expressed in our units as

$$\phi_t = \Phi(r_t)/\sigma^2 = -9\mu/C \quad (16)$$

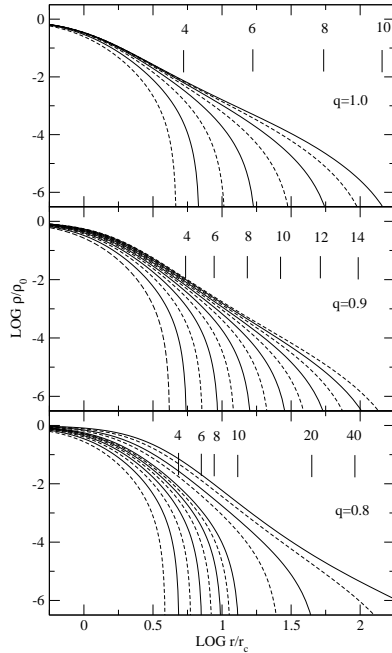


Fig. 2. Mass density profiles for three representative models. The upper panel correspond to a  $q = 1$  model which is exactly the standard Michie-King models. The other two panels correspond to models with  $q = 0.9$  and  $0.8$  respectively. We can see that models having the same size in units of  $r_c$ , but different values of  $q$ , show a large variety of density profiles. In each panel it is also indicated the corresponding  $-\phi_0$  of each model.

and this value can be used as a correction to be added in order to find the gravitational potential at the center. As a final step, the corrected potential can be used to estimate the potential energy

$$U = \frac{1}{2} \int_0^{r_t} 4\pi\Phi\rho r^2 dr = \frac{GM}{r_t} \nu \quad (17)$$

where

$$\nu = \frac{C}{18\mu^2} \int_0^C \phi r^2 dr. \quad (18)$$

In Tables 1 and 2 we show the major parameters obtained in this class of lowered models. The first column present the uncorrected central potential,  $\phi_0$ , used to start the integration of the model. The radius containing half the mass,  $r_h$ , is shown in column 2 in units of the core radius. For the King model,  $q = 1$ , the half radius is relatively stable even considering the large variation covered by the concentration index. We see that the tidal radius,  $r_t$ , varies by more than two orders of magnitudes while the half radius is kept almost fixed

$-\phi_0$	$r_h/r_c$	$\mu$	$\phi_t$	Log C	$\nu$	$C_1$	$C_2$
q=1.0							
-2	0.567	0.224	-0.631	0.505	1.399	1.609	1.486
-3	0.651	0.413	-0.790	0.672	1.565	1.641	1.527
-4	0.701	0.645	-0.840	0.840	1.803	1.688	1.587
-5	0.729	0.941	-0.791	1.030	2.178	1.760	1.678
-6	0.744	1.346	-0.673	1.255	2.733	1.880	1.821
-7	0.751	1.985	-0.529	1.528	3.489	2.141	2.036
-8	0.755	3.178	-0.419	1.834	4.166	2.512	2.241
-9	0.757	5.569	-0.381	2.119	4.176	2.883	2.217
-10	0.757	10.019	-0.403	2.350	3.702	2.772	2.064
q=0.9							
-2	0.579	0.224	-0.662	0.484	1.360	1.600	1.475
-3	0.679	0.410	-0.875	0.625	1.472	1.620	1.501
-4	0.751	0.629	-1.012	0.748	1.612	1.643	1.533
-5	0.806	0.880	-1.083	0.864	1.786	1.670	1.570
-6	0.850	1.165	-1.096	0.981	2.006	1.701	1.615
-7	0.888	1.487	-1.063	1.100	2.283	1.738	1.670
-8	0.920	1.852	-0.993	1.225	2.638	1.783	1.738
-9	0.950	2.274	-0.897	1.358	3.095	1.837	1.825
-10	0.978	2.771	-0.785	1.502	3.685	1.908	1.938
-11	1.003	3.375	-0.667	1.658	4.448	2.005	2.093
-12	1.029	4.142	-0.552	1.830	5.408	2.148	2.309
-13	1.053	5.171	-0.451	2.014	4.678	2.378	2.599
-14	1.076	6.625	-0.373	2.204	7.542	2.774	2.909

at 70% of the core radius. For the other models this stability of the half radius is not generally preserved. As an example, for a model with  $q = 0.9$  a similar variation of the concentration index would imply in a variation of a factor of two on the half radius. Actually, models with lower  $q$  index show a more important departure from the Maxwellian case since the variation of the half radius is even larger. This large variation in the half radius is a consequence

$-\phi_0$	$r_h/r_c$	$\mu$	$\phi_t$	Log C	$\nu$	$C_1$	$C_2$
q=0.8							
-2	0.588	0.225	-0.688	0.468	1.329	1.594	1.467
-3	0.699	0.409	-0.942	0.592	1.407	1.607	1.484
-4	0.784	0.626	-1.144	0.692	1.494	1.620	1.503
-5	0.855	0.869	-1.300	0.779	1.589	1.633	1.522
-6	0.915	1.137	-1.418	0.858	1.695	1.647	1.542
-7	0.969	1.427	-1.503	0.932	1.811	1.660	1.562
-8	1.017	1.737	-1.560	1.001	1.939	1.673	1.583
-9	1.062	2.067	-1.595	1.067	2.078	1.686	1.604
-10	1.104	2.417	-1.609	1.131	2.231	1.698	1.626
-15	1.286	4.438	-1.490	1.428	3.247	1.760	1.742
-20	1.442	6.934	-1.193	1.719	4.949	1.820	1.881
-30	1.708	14.190	-0.471	2.434	15.604	2.023	2.562
-40	1.936	50.098	-0.139	3.510	31.581	17.164	3.918

Resume of the lowered model parameters. The upper panel,  $q = 1$ , shows the same solution as founded with the King models. The other panel illustrate the effect of changing the  $q$  non extensivity parameter on the structural parameter.

of a change in the shape of the density profile for these models as can be seen from figures 1 and 2. In fact, these figures show that for a similar external radius the gradient in the density profile is different for each value of  $q$ .

In the last two columns of Tables 1 and 2 we present two concentration indices based only on the projected surface density distribution. They are based in the radii containing respectively 1/4, 1/2 and 3/4 of the total mass in each model. The concentration index  $C_1$  is defined to be equal to  $r_{1/2}/r_{1/4}$  and therefore measure the degree of concentration in the central mass distribution. On the other hand the index  $C_2$  is estimated as  $r_{3/4}/r_{1/2}$  and measure the spread of the mass distribution of the outer region. These two indices are useful to give a broad representation of the gamma of variations seen in the surface density profiles for these models. For a single parameter family each profile is represented as one single point in the  $C_1, C_2$  plane. This feature is illustrated in figure 4 for each model represented in Tables 1 and 2. For a given value of  $q$  the models falls in a line representing the gross features of the individual profiles. Along each line  $q$  line the position of the points are uniquely determined by the parameter  $-\phi_0$ . On the other hand these same plots can be easily obtained from luminosity observed profiles. Therefore we can use the points in this

plane to give a gross diagnostic of the models more appropriated to each class of objects. Observe that all models tend to converge to a single point for low  $-\phi_0$  models, independent of the  $q$  index. This is a consequence of the density profile as a function of the potential as shown in figure 1. For low values of  $-\phi_0$  the profiles tend to approximate a polytropic with  $n = 5/2$ . As a consequence, these models tend to present a unique surface density profile and therefore also have a unique pair of concentration indices  $C_1 \simeq 1.46$  and  $C_2 \simeq 1.28$ . This regime coincides with the profiles of highly tidally affected models where the tidal radius is closer to the core radius. Therefore, strongly tidally truncated GC tend to be equally well represented by different  $q$  models. However, when we begin to sample larger values of the central potential we observe the differences among the  $q$  models. In this regime the individual density profiles behaves quite differently as a function of the parameter  $q$ .

The King models, represented here by the subclass with  $q = 1$ , are known to give a good representation of the globular clusters. An empirical fit to the radial distribution of GC show that (Djorgovski & Meylan 1994)

$$\rho(r) = \rho_0 \left(1 + \frac{r}{r_c}\right)^{-\alpha} \quad (19)$$

with  $3.5 < \alpha < 4$ . Using this empirical description we indicate in Figure 4 the region corresponding to the GC profiles by the letter G. We can see that models having  $\alpha = 3.5$  tend to fall quite close to the region described by the King models. At this point one may ask if these q-lowered models may provide at least a reasonable description for elliptical galaxies. Such a possibility will be examined next section.

#### 4 Profiles For Elliptical Galaxies

The density profile of elliptical galaxies have been widely investigated either from the observational and theoretical point of view. A very successful approach consist in represent the luminosity profile of these objects by  $r^{1/4}$ , usually termed de Vaucoulers law (de Vaucoulers 1948; de Vaucoulers & Capaccioli 1979). Although existing many indications that such empirical relation is not universal, there is a firm believe that it provides a good representation for several elliptical galaxies.

A generalization of the de Vaucoulers law is the so-called Sérsic law where the luminosity profiles are represented by an expression,

$$I_r = I_e 10^{-b_n \left[\left(\frac{r}{r_e}\right)^{1/n} - 1\right]} \quad (20)$$

where  $n$  is the Sérsic index and  $b_n$  is a properly defined constant so that the effective radius  $r_e$  contains half of the total luminosity. In particular, for  $n = 4$  the de Vaucouleurs profile is recovered. Models with  $n \simeq 3$  can be represented by the lowered King models, but those with  $n \simeq 4$  are definitely better represented by a model with  $0.9 < q < 1$ .

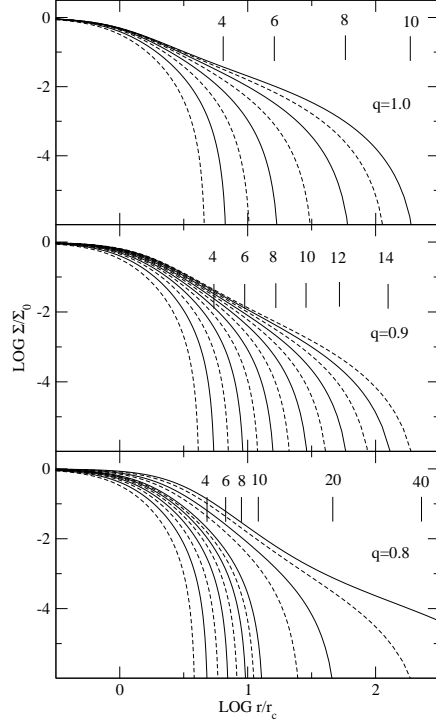


Fig. 3. Projected density profiles for the 3 classes of models presented in Figure 2. Models corresponding to lower values of  $-\phi_0$ , and hence  $C$ , have a higher similarity due to the dominant effect of the external polytropic structure ( $n = 5/2$ ).

A simple integration of the de Vaucouleurs law leads to profile corresponding to a pair of concentrations indexes  $C_1 = 2.730$  and  $C_2 = 2.506$ , which is represented by the label  $r^{1/4}$  in figure 4. It is interesting to observe that this point is closely represented by a model  $q \simeq 0.95$  and  $-\phi_0 \simeq -10.45$ . In figure 5 we present the projected density profile corresponding to this model. As one may see, this model is a good representation of the de Vaucouleurs law over an interval of nearly 10 orders of magnitudes. There are two points that deserve a further comment. The first one is that models with parameters  $q \simeq 0.95$  and  $\phi = -10.45$  are the best representation of the de Vaucouleurs law. If we explore the parameter region neighboring this point we can verify that the agreement is progressively lost. In figure 4 we illustrate that point by exploring points departing 1% from that optimum model.

The other point of interest is that our representation of the de Vaucouleurs law does not exactly reproduce the  $r^{1/4}$  profile. There is a noticeable oscillation around that trend. Over the 10 magnitude interval were the  $q$  profile is close to

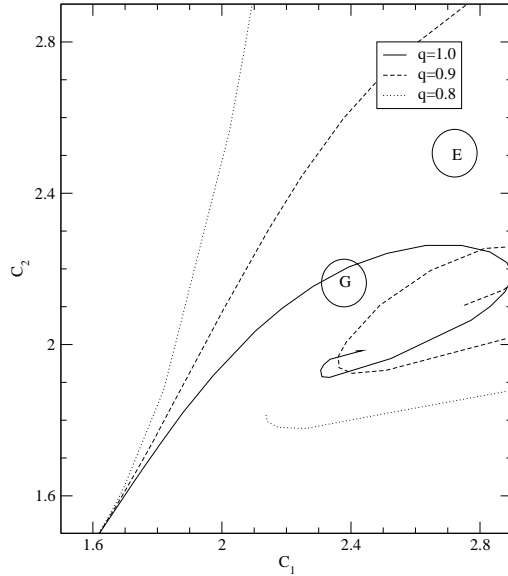


Fig. 4. This concentration diagram shows the gross characteristic of the mass distribution as a response in changing the  $q$  nonextensive parameter. The interrupted line with the label G mark the approximated location of GC lying close to the King model, corresponding to  $q = 1$ . The circular region with the label  $r^{1/4}$  law marks the position of the elliptical galaxies obeying the de Vaucouleurs law. In this case, a good description of the luminosity profile is provided by a model with  $q = 0.95$ .

the de Vaucouleurs law this oscillations have an amplitude of the order of 0.2 magnitudes. The remarkable fact is that the same phenomenon was observed by Caon (Caon *et al.* 1997) in the elliptical galaxies belonging to the Virgo cluster. This is clearly a point that deserve a closer scrutiny in the future.

## 5 Conclusion

In this paper we have proposed a new family of lowered models with basis on the nonextensive kinetic theory. As we have seen, these  $q$ -lowered models based on Tsallis statistics extend naturally the class of Michie-King family and are also able to reproduce the observed structure of globular clusters. Although giving a broader range of density profiles than the usual King-Michie lowered models, the region occupied by these system in the concentration index diagram remains close to the  $q = 1$  models which correspond exactly to the classical King models. It remains a matter of investigation to verify if the actual observed profiles of galactic globular clusters do favor a  $q = 1$

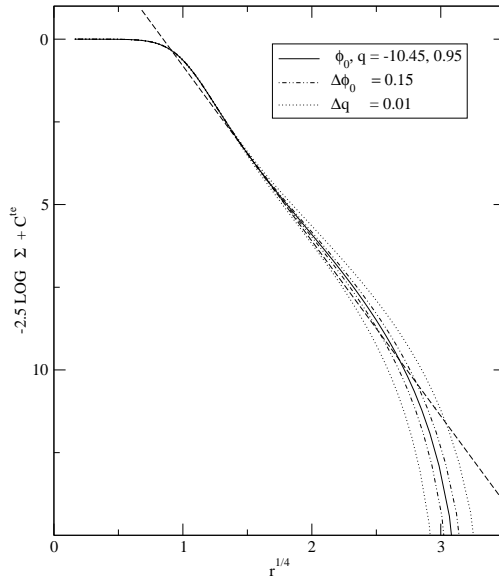


Fig. 5. A comparison of the  $q = 0.95$  model with the de Vaucouleurs law showing that this model may give a good description of the  $r^{1/4}$  law over an interval of 10 magnitudes.

lowered Maxwellian distribution or if there exist room do discuss the presence of departures from this solution.

For elliptical galaxies the situation is much more favorable to the nonextensive models. It is known that the Michie-King models do not give a close representation of the observed profiles of elliptical galaxies. Some objects, like NGC 4472, possibly affected by tidal truncation are well represented by the King profile (King 1978). However, the vast majority of bright elliptical, as NGC 3379, do not fit quite well in the King model and tend to be closer to the de Vaucouleurs profile (de Vaucouleurs & Capaccioli 1979). In this concern, the contribution of the lowered nonextensive models can be quite important since it is possible to find models which are closely resembling the structure of elliptical galaxies. In fact a model with  $q = 0.95$  is able to reproduce the de Vaucouleurs empirical law over more than 10 magnitudes of surface brightness. It could be a matter of great interest to pursue a more detailed comparison of these models with the actual data on elliptical galaxies. In particular, these non extensive models predict a systematic departure from the de Vaucouleurs law in the central region similar to the findings by Ferrarese (Ferrarese *et al.* 1994). Using data from the Hubble space telescope these authors have demonstrated that the very internal regions of ellipticals tend to show an internal isothermal core quite different from the prediction of a pure

de Vaucouleurs law. Using bright ellipticals in the Virgo cluster they show that the brightness profile become closer to the de Vaucouleurs law only after the inner 10 arcsecond region. There is also a prediction of an external truncation but this could be a more difficult task to detect since this truncation is heavily dependent of the sky subtraction procedure.

## References

- [Abramowitz & Stegun 1972] Abramowitz M., Stegun I.A. 1972, Handbook of Mathematical Functions, Dover, NY.
- [Binney & Tremaine 1994] Binney J., Tremaine S. 1994, Galactic Dynamics, Princeton U. Press, Princeton.
- [Caon *et al.* 1997] Caon N., Capaccioli M. & D’Onofrio M. 1997, MNRAS, **265**, 1021.
- [de Vancoulers 1948] de Vaucouleurs, G. 1948, *Ann. d’Astrophys.*, **11**, 247.
- [de Vancoulers & Capaccioli 1979] de Vaucouleurs G., Capaccioli M. 1979, ApJSS **40**, 699.
- [Djorgovski & Meylan 1994] Djorgovsky S., Meylan G. 1994, AJ **108**, 1292.
- [Ferrarese *et al.* 1994] Ferrarese L., van den Bosch F. C., Ford H. C., Jaffe W., O’Connell R. W. 1994, ApJ, **108**, 1598.
- [Hodge & Michie 1969] Hodge P., Michie R. W. 1969, AJ **74** 587.
- [Jiulin 2007] Jiulin D. 2007, Astrophys. Space Sci. **312**, 47-55.
- [King 1966] King I. R. 1966, Astrophys. J **71**, 64.
- [King 1965] King I. R. 1965, Astrophys. J. **70**, 376.
- [King 1978] King I.R. 1978, Astrophys. J **222**, 1.
- [King 1981] King I. R. 1981, QJRAS **22**, 227.
- [King 1962] King I. R. 1962, Astron. J. **67**, 471.
- [Lavagno *et al.* 1998] Lavagno A., Kaniadakis G., Rego-Monteiro M., Quarati P., Tsallis C. 1998, Astrop. Lett. Comm. **35**, 449.
- [Lima *et al.* 2001] Lima J. A. S., Silva R., Plastino A. R. 2001, Phys. Rev. Lett. **86**, 2938.
- [Lima & de Souza 2005] Lima J.A.S., de Souza, R.E. 2005, Physica A **350**, 303-314.
- [Lima *et al.* 2002] Lima J. A. S., Silva R., Santos J. 2002, Astron. Astrophys. **396**, 309-314.
- [Maxwell 1860] Maxwell, J. C. 1860, Philos. Mag. Ser. 4, **20**, 21.
- [Michie 1961] Michie R. W. 1961, ApJ **133**, 781.
- [Michie 1963a] Michie R. W. 1963, MNRAS **125**, 127.
- [Michie 1963b] Michie R. W. 1963, MNRAS **126**, 269.
- [Michie 1963c] Michie R. W. 1963, MNRAS **126**, 331.
- [Michie 1963d] Michie R. W. 1963, MNRAS **126**, 499.
- [Peterson & King 1975] Peterson C. J., King I. R. 1975, ApJ **80**, 427.
- [Peterson 1976] Peterson C. J. 1976, ApJ **81**, 617.

- [Plastino & Plastino 1993] Plastino A., Plastino A. R. 1993, Phys. Lett. A **177**, 177.
- [Spitzer 1987] Spitzer L. 1987, Dynamical Evolution of Globular Clusters, Princeton University Press, New Jersey.
- [Tsallis 1988] Tsallis C. 1988, J. Stat. Phys. **52**, 479.
- [Sau *et al.* 2001] Sau Fa K., Pedron I. T. 2001, arXiv:0108370.
- [Scarfone *et al.* 2008] Scarfone A. M., Quarati P., Mezzorani G., Lissia M. 2008, Astrophys. Space Sci. **315**, 353-359.
- [Silva *et al.* 1998] Silva R., Plastino A. R., Lima J. A. S. 1998, Phys. Lett. A **249**, 401.
- [Taruya & Sakagami 2002] Taruya A., Sakagami M. 2002, Physica A **307**, 185.